

# A Wearable Electrochemical Platform for Noninvasive Simultaneous Monitoring of $\text{Ca}^{2+}$ and pH

Hnin Yin Yin Nyein,<sup>†,‡,§,⊥</sup> Wei Gao,<sup>†,‡,§,⊥</sup> Ziba Shahpar,<sup>†</sup> Sam Emaminejad,<sup>†,‡,§,||</sup> Samyuktha Challa,<sup>||</sup> Kevin Chen,<sup>†,‡,§</sup> Hossain M. Fahad,<sup>†,‡</sup> Li-Chia Tai,<sup>†,§</sup> Hiroki Ota,<sup>†,‡,§</sup> Ronald W. Davis,<sup>||</sup> and Ali Javey<sup>\*,†,‡,§</sup>

<sup>†</sup>Department of Electrical Engineering and Computer Sciences and <sup>‡</sup>Berkeley Sensor and Actuator Center, University of California, Berkeley, California 94720, United States

<sup>§</sup>Materials Sciences Division, Lawrence Berkeley National Laboratory, Berkeley, California 94720, United States

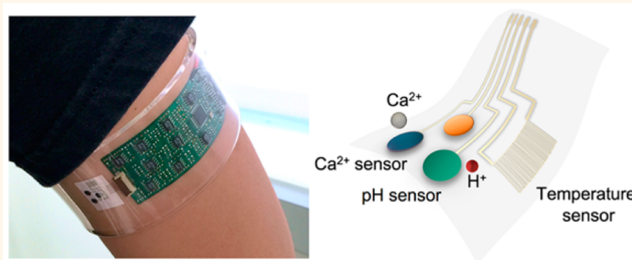
<sup>||</sup>Stanford Genome Technology Center, Stanford School of Medicine, Palo Alto, California 94304, United States

## S Supporting Information

**ABSTRACT:** Homeostasis of ionized calcium in biofluids is critical for human biological functions and organ systems. Measurement of ionized calcium for clinical applications is not easily accessible due to its strict procedures and dependence on pH. pH balance in body fluids greatly affects metabolic reactions and biological transport systems. Here, we demonstrate a wearable electrochemical device for continuous monitoring of ionized calcium and pH of body fluids using a disposable and flexible array of  $\text{Ca}^{2+}$  and pH sensors that interfaces with a flexible printed circuit board.

This platform enables real-time quantitative analysis of these sensing elements in body fluids such as sweat, urine, and tears. Accuracy of  $\text{Ca}^{2+}$  concentration and pH measured by the wearable sensors is validated through inductively coupled plasma-mass spectrometry technique and a commercial pH meter, respectively. Our results show that the wearable sensors have high repeatability and selectivity to the target ions. Real-time on-body assessment of sweat is also performed, and our results indicate that calcium concentration increases with decreasing pH. This platform can be used in noninvasive continuous analysis of ionized calcium and pH in body fluids for disease diagnosis such as primary hyperparathyroidism and kidney stones.

**KEYWORDS:** wearable biosensors, flexible electronics, multiplexed sensing, system integration, in situ analysis



Calcium is an essential component for human metabolism and minerals homeostasis.<sup>1</sup> About 1–2% of human body weight is made up of calcium.<sup>1</sup> Excessive alternation of ionized calcium levels in biofluids can have detrimental effects on the function and structure of many organs and systems in the human body, including myeloma, acid–base balance disorder, cirrhosis, renal failure, and normocalcaemic hyperparathyroidism.<sup>1–3</sup> Free  $\text{Ca}^{2+}$  is usually measured in body fluids, such as urine for estimating kidney stone-forming salts.<sup>2</sup> pH is another crucial component for potential disease diagnosis. For instance, kidney stone patients with type II diabetes are reported to have a lower pH than normal individuals.<sup>4</sup> Change in pH of skin, which is due to sweat, has been reported to take part in the development of skin disorders such as dermatitis, ichthyosis, and fungal infections.<sup>5</sup> Additionally, free  $\text{Ca}^{2+}$  level in biofluids is dependent on pH.<sup>2</sup> Therefore, rigorous processes and rapid analysis of  $\text{Ca}^{2+}$  with pH correction are done in special

laboratories within hours of samples extraction for accurate analysis of biofluids.<sup>2</sup> Such applications can become easier by *in situ* measurement of  $\text{Ca}^{2+}$  and pH in body fluids through a complete data analysis of a reliable wearable sensing platform.

Wearable biosensors have become important for their potential as personal health monitoring systems.<sup>6–15</sup> Recently, multiple research groups have developed wearable devices for real-time monitoring of various electrolytes and metabolites noninvasively using tattoo and textile-based sensors.<sup>6,16–25</sup> Despite recent development of wearable analysis of body fluids, real-time  $\text{Ca}^{2+}$  and pH detections have not been fully explored. Over the past few decades, optical calcium sensors and ion-selective sensors have been developed to study, in general,

Received: June 16, 2016

Accepted: July 5, 2016

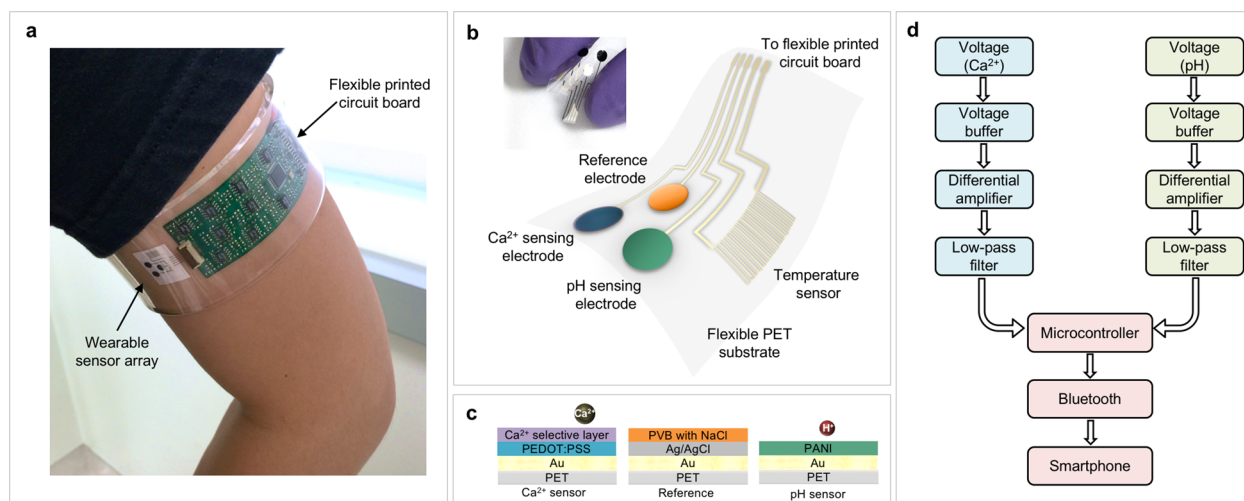


**Figure 1.** (a) A fully integrated wearable multiplexed sensing system on a subject's arm. (b) A schematic of a flexible sensor array containing Ca<sup>2+</sup>, pH, and temperature sensors patterned on a flexible PET substrate. The inset shows a photograph of a flexible sensor array. (c) Surface membrane compositions of a Ca<sup>2+</sup>, a reference, and a pH sensing electrodes. (d) A schematic of a FPCB system for signal conditioning of Ca<sup>2+</sup> and pH sensors (blue and green respectively), data analysis via microcontroller (red), and data transmission to a mobile phone wirelessly via Bluetooth (red).

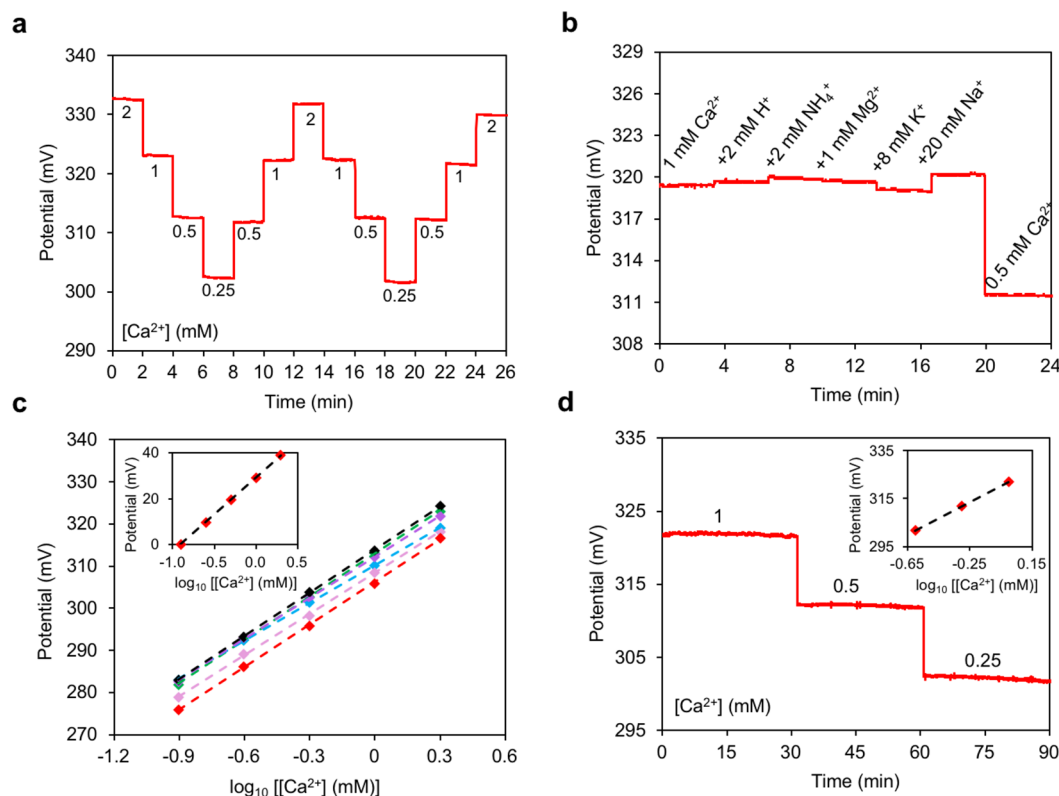


**Figure 2.** General performances of Ca<sup>2+</sup> sensors: (a) sensitivity and repeatability, (b) selectivity, (c) reproducibility of Ca<sup>2+</sup> sensors ( $n = 6$ ), and (d) long-term stability in 0.01 M acetate buffer of pH 4.6. Inset in (c) shows an average linear relationship of  $n = 6$  between open circuit potential and [Ca<sup>2+</sup>] in logarithmic scale. Potentials at 0.25 mM [Ca<sup>2+</sup>] are set to zero. Inset in (d) indicates a linear relationship between open circuit potential and [Ca<sup>2+</sup>] in logarithmic scale.

biological applications,<sup>26–31</sup> but wearable Ca<sup>2+</sup> sensors for health assessment via body fluids have not been studied. On the other hand, careful analysis of the pH of body fluids is needed for more accurate *in situ* measurement.<sup>18,25</sup> The usage of flexible electronics having conformal contact with the human body has fostered more accurate and reliable epidermal quantitative analysis.<sup>6–25</sup> We recently demonstrated a fully

integrated wearable sensing system for real-time multiplexed sensing in human perspiration which allows accurate measurement of sweat analytes through signal processing and calibration.<sup>32</sup> Considering the importance of Ca<sup>2+</sup> and pH and their relationship in body fluids, it is attractive and necessary to simultaneously and selectively measure detailed profiles of Ca<sup>2+</sup> and pH through a fully integrated wearable

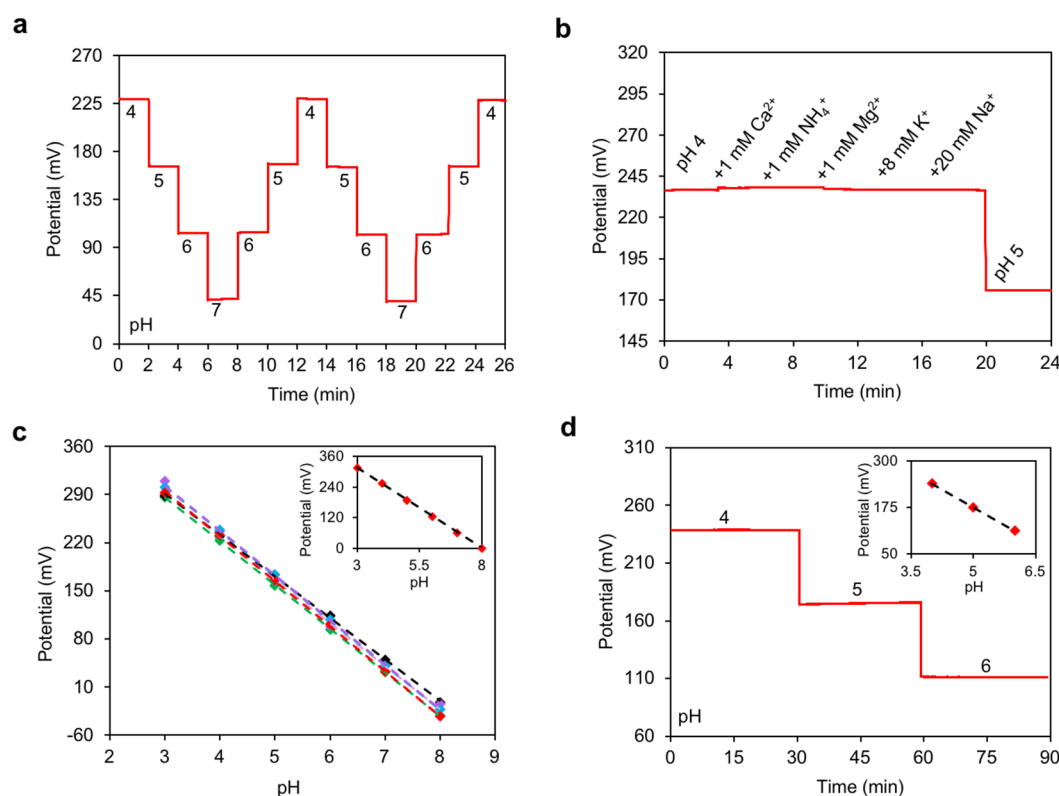


**Figure 3.** General performances of pH sensors: (a) sensitivity and repeatability, (b) selectivity, (c) reproducibility of pH sensors ( $n = 6$ ), and (d) long-term stability in McIlvaine's buffer. Inset in (c) shows an average linear relationship of  $n = 6$  between open circuit potential and pH. Potentials at pH 8 are set to zero. Inset in (d) indicates a linear relationship between open circuit potential and pH.

platform during the course of normal daily activities with real-time feedback.

In this work, we present a wearable sensing system that can real-time monitor  $\text{Ca}^{2+}$  concentration and pH of body fluids as well as skin temperature, using a fully integrated flexible system (Figure 1a). The system allows accurate determination of  $[\text{Ca}^{2+}]$  and pH in body fluids including sweat, urine, and tears. Our system reveals free  $\text{Ca}^{2+}$  concentration and pH by direct measurement of body fluids, such as sweat generated during cycling. Such immediate analysis after fluid secretion minimizes cross-contamination and avoids delayed sample analysis. This also facilitates a closer examination of real-time change in  $\text{Ca}^{2+}$  concentration with pH and reduces the need for pH correction in clinical diagnosis such as hypercalcemia and hypocalcemia tests.<sup>2</sup>

The electrochemical platform consists of a  $\text{Ca}^{2+}$  sensor, a pH sensor, and a skin temperature sensor. These plastic-based biosensors are fabricated on a flexible polyethylene terephthalate (PET) substrate by common physical evaporation and electrochemical deposition methods as illustrated in Figure 1b. Measurements of  $\text{Ca}^{2+}$  concentrations and pH are based on ion-selective electrodes (ISEs), coupled with a polyvinyl butyral (PVB)-coated Ag/AgCl reference electrode (RE). Electrical potential differences between the ISEs and a RE, proportional to the logarithmic concentration of respective target ions, are measured with the aid of the interfacing signal conditioning circuitry. The  $\text{Ca}^{2+}$  sensing electrode consists of a thin organic membrane containing electrically neutral carrier calcium ionophore II (ETH 129)<sup>29</sup> and an ion-electron transducer (PEDOT:PSS),<sup>32</sup> and the pH sensing electrode detects  $\text{H}^+$  by deprotonation at the surface of polyaniline (PANI).<sup>33</sup> The RE is coated with a PVB layer containing saturated NaCl to achieve

a stable potential regardless of ionic strengths of test solutions.<sup>34</sup> Surface membrane compositions of the electrochemical electrodes are demonstrated in Figure 1c. The resistive temperature sensor is based on Cr/Au microlines. The flexible sensor array interfaces with a flexible printed circuit board (FPCB) that includes signal transduction, conditioning, processing, and wireless transmission.<sup>32</sup> As presented in Figure 1d, a differential amplifier is used to measure the voltage output of the  $\text{Ca}^{2+}$  and pH sensors, which is essentially the voltage difference between the PVB-coated shared RE and the ISEs. The high impedance of the ISE-based sensors requires the use of high-impedance voltage buffers in front of the differential amplifier to ensure accurate open circuit voltage measurement. The signal is then passed to a low-pass filter to filter high frequency noise and electromagnetic interferences. The corresponding filtered signals are read and processed further by a microcontroller. The data are then transmitted via Bluetooth to a mobile phone and are displayed on a customized cellphone application.

## RESULTS AND DISCUSSION

Concentration of  $\text{Ca}^{2+}$  in human body fluids commonly varies from 0.5 to 3 mM.<sup>2,35–37</sup> Due to the limited  $\text{Ca}^{2+}$  concentration range, sensitivity is important to ensure accurate measurements. Here, ETH 129 is selected as the  $\text{Ca}^{2+}$ -selective ionophore due to its ability to translocate  $\text{Ca}^{2+}$  across biological membranes.<sup>29</sup> Figure 2a illustrates the general performance of a  $\text{Ca}^{2+}$  sensor in 0.01 M acetate buffer solutions containing 0.25–2 mM  $\text{Ca}^{2+}$ . Dynamic response of the  $\text{Ca}^{2+}$  sensor under consecutive change from high to low and then to high  $\text{Ca}^{2+}$  concentrations is performed two times. Since  $\text{Ca}^{2+}$  is a divalent ion, the ideal

sensitivity of an electrochemical  $\text{Ca}^{2+}$  sensor at standard temperature is 29.6 mV/decade of ion concentration, which is half of a monovalent ion, based upon the Nernst equation.<sup>39,40</sup> The  $\text{Ca}^{2+}$  sensor shows a near-Nernstian response with an average of 32.7 mV/decade in two complete cycles. The sensor shows fast response to changes in  $\text{Ca}^{2+}$  level with a 3.0% relative standard deviation (RSD) of sensitivity. This indicates that  $\text{Ca}^{2+}$  detection by the sensor is reproducible and durable under repetitive testing.

Body fluids contain a variety of electrolytes such as  $\text{Ca}^{2+}$ ,  $\text{Mg}^{2+}$ ,  $\text{Na}^+$ ,  $\text{K}^+$ ,  $\text{H}^+$ , and  $\text{NH}_4^+$ .<sup>35–38</sup> One major requirement of a wearable electrochemical sensor is its ability to selectively discriminate and measure target ions. Thus, it is essential to examine the influence of these major electrolytes on sensor's performance. In this study, interfering ions with physiological relevant concentrations (2 mM  $\text{H}^+$ , 2 mM  $\text{NH}_4^+$ , 1 mM  $\text{Mg}^{2+}$ , 8 mM  $\text{K}^+$ , and 20 mM  $\text{Na}^+$ ) are subsequently added into 1 mM  $\text{Ca}^{2+}$  solution, and measurements are done after 20 s waiting time. The change in potential due to addition of such ions, as demonstrated in Figure 2b, is significantly smaller than the response for typical physiological  $[\text{Ca}^{2+}]$  variations (e.g., 1 mM to 0.5 mM). This shows that the sensor is selectively responsive to  $\text{Ca}^{2+}$  and hence makes it feasible for body fluid analysis. Additionally, it is important that sensors should be reproducible such that reliable analysis can be attained from individual sensors. Six sample sensors were tested in a solution containing 0.125–2 mM of  $\text{Ca}^{2+}$  concentration range. As displayed in Figure 2c, the absolute potentials of these six sensors range from 275.9 to 283.0 mV in the presence of 0.125 mM  $\text{Ca}^{2+}$ . These sensors show sensitivity ranging from 29.8 to 34.2 mV/decade of concentration, with an average sensitivity of 32.2 mV/decade and a RSD of 1.5%. The value of average sensitivity is used as a standard slope for calibration in later studies of biofluids. The variations in the absolute potentials of different sensors (resulted from sensor preparations and manually drop-casting method) are resolved by one-point calibration, as shown in inset of Figure 2c, in which the open-circuit potential of the sensors in 0.125 mM  $\text{Ca}^{2+}$  is set to zero by the microcontroller. This is similar to commercial pH meters where a standard solution is used to calibrate the measurement before actual measurement is undertaken. In the case of long-term analysis on  $\text{Ca}^{2+}$  concentration in body fluids, variation due to potential drift can easily conceal the actual measurement results. To test this, the  $\text{Ca}^{2+}$ -selective sensor is kept under 0.25–1 mM  $\text{Ca}^{2+}$  solutions for a total of 90 min and under 1 mM solution for 4 h as presented in Figures 2d and S1, respectively. A sensitivity of 33.7 mV/decade is measured in Figure 2d, and a potential drift of 1.1 mV/h is observed in Figure S1. These results reveal that the  $\text{Ca}^{2+}$  sensors can yield a small error of approximately 8% over an hour of continuous measurement without large deviation from the average sensitivity.

Similar to the  $\text{Ca}^{2+}$  sensors, general performances of the pH sensors are evaluated. PANI has been a popular medium for pH measurement in body fluids due to its ease of fabrication, reproducibility, and biocompatibility.<sup>18,25</sup> In this study,  $\text{H}^+$ -selective PANI film is electrochemically deposited onto a Au electrode by cyclic voltammetry. The resulting PANI-based pH sensor presented in Figure 3a was tested repeatedly in McIlvaine's buffer from pH 4 to 7. Results exhibited an average slope of 62.5 mV/decade with RSD 1.0% in two complete cycles from pH 4 to 7 and then to 4 with one-unit increments. The pH sensor is also selective to  $\text{H}^+$  with a potential variation of approximately 3.1% compared to its sensitivity as shown in

Figure 3b. Since pH in human body fluids commonly fluctuates between 3 and 8 depending on specific fluids,<sup>3–5,41</sup> sensors are characterized from pH 3 to 8. Reproducibility of six sensors is reported in Figure 3c. Results show that absolute potentials range from 285.6 to 309.8 mV at pH 3 and sensitivities vary from 60.0 to 65.4 mV/decade of concentration. Regardless of the variation in absolute potentials, these sensors show only a RSD of 2.3% in sensitivity with a 63.3 mV/decade average. This average sensitivity is later used as a standard calibration value for measurement in body fluids. Long-term performance of the pH sensor is captured in Figures 3d and S1. The results in Figure 3d show that sensitivity of pH sensor is 63.7 mV/decade over a 90 min measurement. Figure S1 indicates that deviation due to potential drift is 0.7 mV/h which corresponds to 1.1% error in pH value over an hour of continuous measurement. Previously reported wearable pH sensors are not sufficiently accurate for detailed quantitative analysis in body fluids due to  $\text{Cl}^-$  influence on solid-state Ag/AgCl RE.<sup>18,25,42</sup> Here, pH sensing with Ag/AgCl and PVB-based Ag/AgCl REs is compared under a constant pH 5.0 with varying  $\text{Cl}^-$  concentrations. Figure S2 depicts that variation of  $\text{Cl}^-$  concentration greatly influences the performance of the sensor with Ag/AgCl RE, while that with PVB-based RE remains relatively stable. This is because the PVB layer contains  $\text{Cl}^-$  and is immune to change in  $\text{Cl}^-$  concentrations. The above results exhibit that present pH sensors provide an accurate and reliable analysis capability compared to previously reported electrochemical pH sensors.

Skin temperature is an effective marker of the thermal state of individuals and is also informative for many skin related diseases (such as ulceration).<sup>43</sup> General performance of the Cr/Au-based temperature sensors was evaluated previously in our recent work.<sup>32</sup> These resistive temperature sensors have a sensitivity of 0.18% per  $^\circ\text{C}$  with respect to its baseline resistance at room temperature. To investigate the influence of temperature on  $\text{Ca}^{2+}$  and pH sensors, sensors are tested in temperatures ranging from 23 to 37  $^\circ\text{C}$  in McIlvaine's buffer of pH 5.0 containing 0.5 mM  $\text{Ca}^{2+}$ . Unlike enzymatic sensors in which the performance is greatly influenced by the change in temperature,<sup>32</sup> both  $\text{Ca}^{2+}$  and pH sensors show no significant response to temperature change as illustrated in Figure S3.

In order to ensure accurate measurement of body fluids,  $\text{Ca}^{2+}$  and pH analyses of human sweat and urine samples using the wearable sensors are validated with inductively coupled plasma-mass spectrometry (ICP-MS) technique and a commercial pH meter, respectively. Measurements of biofluids using sensors are computed based on a calibration curve obtained from artificial body fluids (detailed in the Experimental Section). Results displayed in Table 1 show  $\text{Ca}^{2+}$  concentrations and pH in sweat and urine measured by ICP-MS and  $\text{Ca}^{2+}$ -selective sensors. Measurements of sweat and urine  $[\text{Ca}^{2+}]$  acquired by sensors vary by a maximum of 7.0% and 10%, respectively, from the ICP-MS results. On the other hand, pH sensors show <2.2% and 3.6% variations in sweat and urine from a commercial pH meter. These variations are relatively small, compared to normal range of  $[\text{Ca}^{2+}]$  and pH of body fluids.

To further confirm the accuracy of sensor readings, additional studies were made by adding fixed amounts of  $\text{Ca}^{2+}$  and  $\text{H}^+$  into raw sweat, urine, and tear samples, and the change in potential with concentration was examined. Figure 4a–c presents a change in potential upon addition of  $\text{Ca}^{2+}$  in urine, tear, and sweat, respectively. These measurements lie along a standard calibration line obtained in Figure 2c with a



**Table 1.**  $\text{Ca}^{2+}$  Concentrations in Sweat and Urine Measured by  $\text{Ca}^{2+}$ -Selective Sensors and ICP-MS and pH of Sweat and Urine Measured from a Commercial pH Meter and pH Sensors

|         | [ $\text{Ca}^{2+}$ ] (mM) |        | pH        |          |
|---------|---------------------------|--------|-----------|----------|
|         | $\text{Ca}^{2+}$ sensor   | ICP-MS | pH sensor | pH meter |
| sweat 1 | 0.96                      | 0.92   | 4.4       | 4.5      |
| sweat 2 | 0.48                      | 0.48   | 7.2       | 7.3      |
| sweat 3 | 0.76                      | 0.71   | 8.1       | 8.1      |
| urine 1 | 1.8                       | 1.8    | 7.6       | 7.8      |
| urine 2 | 7.2                       | 7.1    | 6.3       | 6.5      |
| urine 3 | 1.2                       | 1.1    | 6.4       | 6.6      |

slope of 32.2 mV/decade. Such a method provides an alternate mean to verify the sensors' measurement accuracy. Due to the buffering capacity of body fluids, the actual pH of the solutions is measured with a commercial pH meter after every  $\text{H}^+$  addition to raw urine, tears, and sweat samples. Measured pH results in urine, tears, and sweat are plotted against the potentials in Figure 4d–f. Similar to the  $\text{Ca}^{2+}$  sensors, measurements of pH sensors lie nearly along the calibration line with a slope of 63.3 mV/decade. The study confirms that

complex body fluids have minimal interference with sensors' readings.

Following the *ex situ* analysis of sweat, urine, and tear, real-time on-body evaluation in human perspiration using the flexible integrated wearable device was also performed. As illustrated in Figure 5a, a subject wears a headband embedded with the fully integrated flexible sensing system while cycling. Real-time analysis is then wirelessly transmitted to a mobile phone and displayed in a custom-developed cellphone application. On-body assessment of sweat  $\text{Ca}^{2+}$  and pH was performed with a 5 min ramp-up and a 20 min biking at a power of 150 W, followed by a 5 min cool-down session (Figure 5b). Sweat is simultaneously collected for analysis using ICP-MS and a commercial pH meter. Figure 5c shows change in skin temperature with exercise time. Initially, the temperature increases as exercise progresses, and a trough in the measurement curve is observed between 6 and 11 min of cycling time. This indicates that perspiration begins and initiates the measurements of other ion-selective sensors. Temperature then remains stable in the rest of the cycling time. This behavior is consistent with our previously reported work.<sup>32</sup> Figure 5d depicts real-time sweat pH profile with exercise time. Initially, the sensors have no response during the first 10 min because there is not enough sweat generated. After

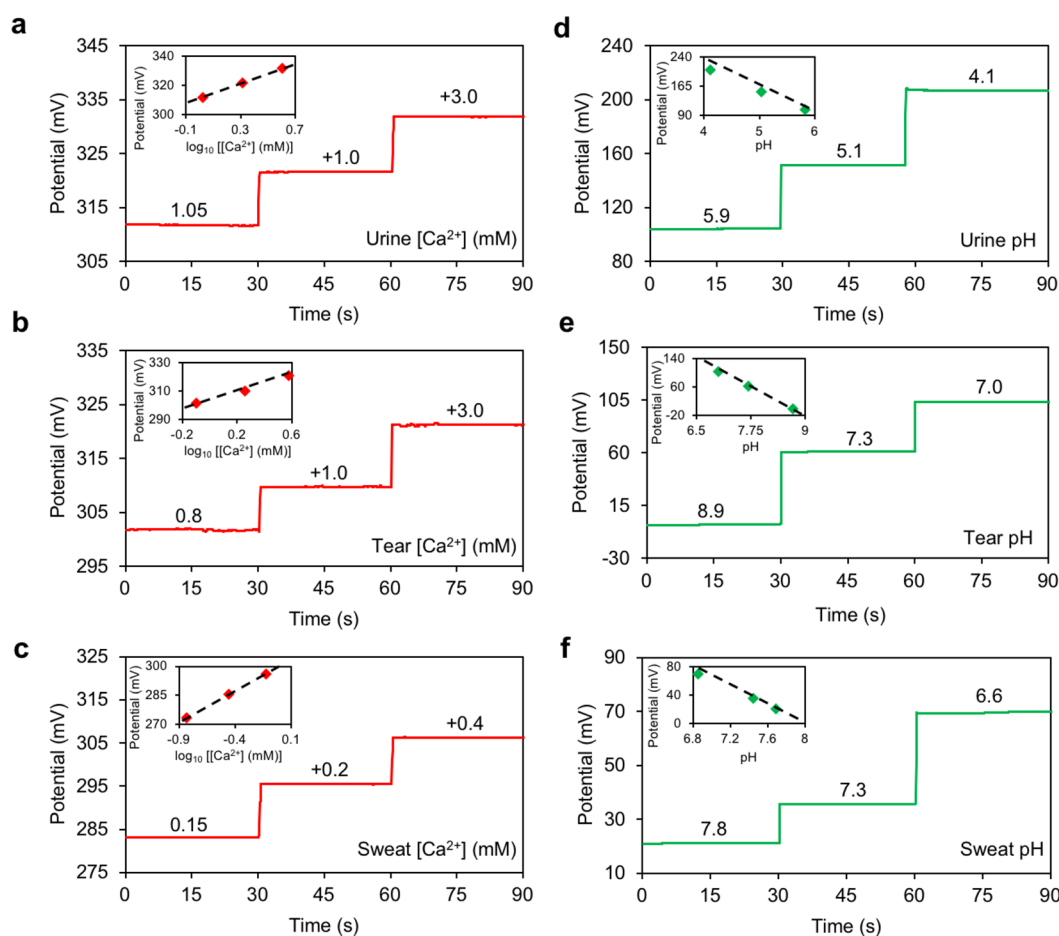


**Figure 4.** Off-body evaluations of  $\text{Ca}^{2+}$  (a–c) and pH (d–f) sensors in urine (a, d), tear (b, e), and sweat (c, f). Measurements of  $[\text{Ca}^{2+}]$  are done by consecutively adding  $\text{Ca}^{2+}$  into raw biofluids. The amounts added are indicated in the figures. Measurements of pH are done by consecutively adding HCl into raw biofluids. The final pH is determined by a commercial pH meter. Linear regression lines in inset figures correspond to sensors' responses in standard calibration solutions obtained in Figure 2c for  $\text{Ca}^{2+}$  measurement and in Figure 3c for pH measurement.

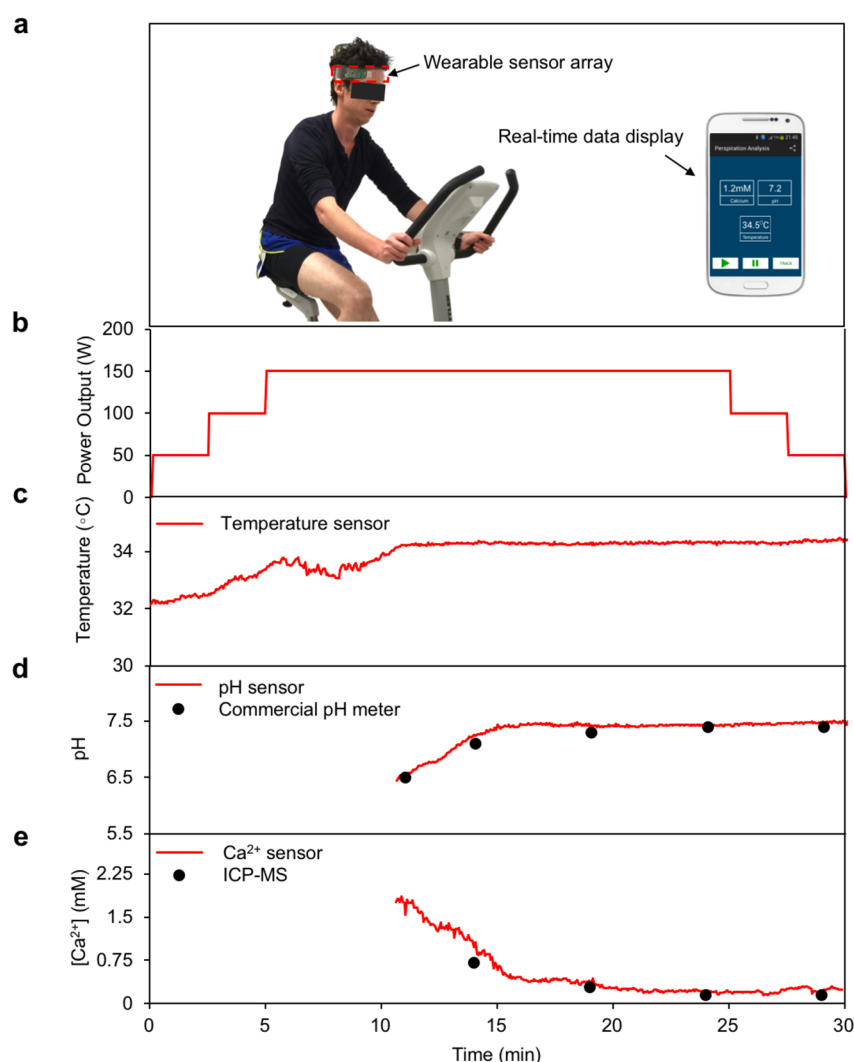


**Figure 5.** Real-time on-body analysis of human perspiration during a constant-load cycling. (a) A wearable multiplexed sensing system is worn on a subject's forehead during stationary cycling, and data are directly read in a customized application and saved in a mobile phone. (b) Subject's cycling power output and real-time sweat analysis results of (c) skin temperature, (d) pH, and (e)  $\text{Ca}^{2+}$  concentration using a fully integrated wearable sensing system. Black dots in (d and e) correspond to measurements done by a pH meter and by ICP-MS, respectively.

10 min into cycling, sweat pH is observed to increase gradually for 5 min which is mainly due to a decrease of lactic acid concentration in sweat.<sup>32</sup> Sweat pH then stabilizes in the remaining 15 min of exercise. This on-body result had close readings with a commercial pH meter. In Figure 5e, the  $\text{Ca}^{2+}$  sensor shows an opposite trend compared to pH. Concentration of  $\text{Ca}^{2+}$  initially decreases rapidly with increasing pH and stabilizes after 15 min. ICP-MS result also shows a similar trend with slightly lower concentrations than the on-body readings. This result is consistent with literature which reports an inverse relation between concentration of  $\text{Ca}^{2+}$  and pH.<sup>2</sup> These on-body results further affirm the utilization of the wearable system in personal health care. Such real-time continuous analysis can alert the wearer regarding excessive loss or rise of electrolytes.

## CONCLUSION

In conclusion, we have developed a fully integrated wearable electrochemical platform for simultaneous *in situ* analysis of  $\text{Ca}^{2+}$  and pH in body fluids. The wearable system, containing flexible sensors coupled with integrated circuits and a wireless

transceiver, enables accurate measurements of biofluids, including urine, tear, and sweat with real-time feedback. The study emphasizes the practical applications of wearable sensing systems as a simplification of the traditional extensive laboratory analysis for accurate measurement of analytes in complex biofluids. The sensors' capabilities for long-term quantitative analysis and real-time on-body monitoring can also provide insightful information about  $\text{Ca}^{2+}$  and pH homeostasis in the human body. Owing to its miniaturization, system integration, and measurement simplification, the proposed platform manifests a useful wearable sensing system that can be exploited for disease diagnosis where rapid analysis is desired for  $\text{Ca}^{2+}$  and pH in body fluids. Future efforts toward a reliable sensing system will focus on minimizing potential drifts and performance variations for large-scale population-based investigations to further understand the physiological states of individuals.

## EXPERIMENTAL SECTION

**Materials.** Calcium ionophore II (ETH 129), bis(2-ethylexyl) sebacate (DOS), sodium tetrakis[3,5-bis(trifluoromethyl)phenyl] borate (Na-TFPB), high-molecular-weight polyvinyl chloride (PVC),

tetrahydrofuran (THF), polyvinyl butyral resin BUTVAR B-98 (PVB), sodium chloride (NaCl), 3,4-ethylenedioxythiophene (EDOT), poly-(sodium 4-styrenesulfonate) (NaPSS), and aniline were purchased from Sigma-Aldrich (St. Louis, MO). Moisture-resistant 100  $\mu\text{m}$ -thick PET was purchased from McMaster-Carr (Los Angeles, CA). All reagents were used as received.

**Fabrication of Electrodes Array.** The fabrication process is the same as our previously reported work.<sup>32</sup> In brief, PET was cleaned with isopropyl alcohol and  $\text{O}_2$  plasma etching. An electrode array of 3.2 mm in diameter was patterned via photolithography and was thermally evaporated with 30/50 nm of Cr/Au, followed by lift-off in acetone. The electrode array was additionally coated with 500 nm parylene C insulation layer in a SCS Labcoter 2 Parylene Deposition System, and the 3 mm-diameter sensing electrode area was defined via photolithography. The fabricated array was further etched with  $\text{O}_2$  plasma to remove the parylene layer at the defined sensing area. Finally, 200 nm Ag was deposited via thermal evaporation and lift-off in acetone.

**Preparation of  $\text{Ca}^{2+}$  Selective Sensors and pH Sensors.**  $\text{Ca}^{2+}$ -selective cocktail was prepared by dissolving 100 mg of 33:0.5:65.45:1 wt % ratio of PVC:NaTFPB:DOS:ETH129 in 660  $\mu\text{L}$  THF. Surface of the  $\text{Ca}^{2+}$ -selective electrodes was modified by galvanostatic electrochemical polymerization of 0.01 M EDOT with 0.1 M NaPSS at a constant current of 2  $\text{mA}\cdot\text{cm}^{-2}$  to produce polymerization charges of 10 mC. Ten  $\mu\text{L}$  (1.4  $\mu\text{L}\cdot\text{cm}^{-2}$ ) of  $\text{Ca}^{2+}$ -selective cocktail was then drop-casted onto a PEDOT:PSS coated electrode and left to dry overnight in a dark environment. Aniline was distilled at a vapor temperature of 100  $^\circ\text{C}$  and a pressure of 13 mmHg before usage. It should be pointed out that a freshly distilled aniline solution should be used within a week. PANI was polymerized in a 0.1 M aniline/0.1 M HCl solution. Au surface was first modified by depositing Au (50 mM  $\text{HAuCl}_4$  and 50 mM HCl) for 30 s at 0 V, followed by PANI deposition using cyclic voltammetry from  $-0.2$  to 1 V for 25 cycles at 100 mV/s.

**Evaluation of  $\text{Ca}^{2+}$  and pH Sensors General Performances.** General performance of  $\text{Ca}^{2+}$  sensors was tested under a 0.01 M acetate buffer solution (pH 4.6) containing varying  $\text{Ca}^{2+}$  concentrations unless stated otherwise. Interference study was performed by subsequent addition of chloride solutions containing various cations (2 mM  $\text{H}^+$ , 2 mM  $\text{NH}_4^+$ , 1 mM  $\text{Mg}^{2+}$ , 8 mM  $\text{K}^+$ , and 20 mM  $\text{Na}^+$ ) into a 1 mM  $\text{Ca}^{2+}$  solution. pH sensors were tested using McIlvaine's buffer with varying pH to characterize general performances of the sensors. Interference study was conducted by subsequent addition of chloride solutions containing 1 mM  $\text{Ca}^{2+}$ , 1 mM  $\text{NH}_4^+$ , 1 mM  $\text{Mg}^{2+}$ , 8 mM  $\text{K}^+$ , and 20 mM  $\text{Na}^+$  into a McIlvaine's buffer solution of pH 4.0. All measurements were paused while changing solutions, and measurements were done after 20 s waiting period.

**Ex Situ Evaluation of Body Fluids.** Urine, sweat, and tear samples were collected from volunteer subjects for off-body evaluation. Sweat and urine were initially tested with ICP-MS to measure  $[\text{Ca}^{2+}]$ , and the results were compared with the sensor readings of same sweat and urine samples. Sweat samples were diluted four times with deionized water for *ex situ* evaluations using ICP-MS and wearable sensors. The results were converted back in Table 1 to reflect raw sweat  $\text{Ca}^{2+}$  concentrations.  $[\text{Ca}^{2+}]$  measured by the sensor was computed using a calibration curve. The calibration curve was obtained from artificial body fluids containing 50 mM NaCl and 4 mM KCl with 0.25, 0.5, and 1 mM  $\text{CaCl}_2$  in 0.01 M acetate buffer. pH of the samples was measured with a commercial pH meter (Horiba LAQUA Twin pH meter B-713) and PANI-based pH sensors. PANI-based pH sensor measurement was obtained by using similar methods as the  $[\text{Ca}^{2+}]$  measurement. pH values were computed from a calibration curve obtained from solutions containing 50 mM NaCl and 4 mM KCl with McIlvaine buffer of pH varying from 4 to 7. To further confirm sensor readings, raw sweat, urine, and tear samples were subsequently added with a fixed amount of  $\text{Ca}^{2+}$ , and initial  $[\text{Ca}^{2+}]$  was back-calculated based on the change in potential with concentration. The relationship between potential change and logarithmic concentration was analyzed by comparing with a standard calibration curve obtained from Figure 2c. As in measuring  $[\text{Ca}^{2+}]$ , HCl was

subsequently added into the original body fluids, and final pH was verified by a commercial pH meter and compared with PANI-based sensor readings. In this case, a pH meter due to buffering capacity of body fluids measured the actual pH of the body fluids. The measured pH results were compared with a standard calibration line obtained from Figure 3c.

**In Situ Assessment of Sweat  $[\text{Ca}^{2+}]$ , pH, and Skin Temperature.** On-body evaluation of sweat  $[\text{Ca}^{2+}]$  and pH was performed in compliance with the protocol that was approved by the institutional review board at the University of California, Berkeley (CPHS 2014-08-6636). Five healthy male subjects, aged 20–30, were recruited from the University of California, Berkeley campus. All subjects gave written, informed consent before participating in the study. An electronically braked leg-cycle ergometer (Kettler E3 Upright Ergometer Exercise Bike) was used for stationary cycling trials. Subjects were told to bike for 30 min at a constant workload cycle ergometry. Subject's forehead was wiped and cleaned with alcohol swab and gauze prior to wearing the sensor. Cycling protocol included a 5 min ramp-up and a 20 min biking at a power of 150 W, followed by a 5 min cool-down session. Data are directly recorded in a mobile phone via a customized application. Sweat was simultaneously collected every 5 min during cycling to compare on-body data with measurements from the ICP-MS and a pH meter. Collected sweat was diluted four times for ICP-MS measurements.

## ASSOCIATED CONTENT

### Supporting Information

The Supporting Information is available free of charge on the ACS Publications website at DOI: 10.1021/acsnano.6b04005.

Figures S1–S3 as referenced in the paper (PDF)

## AUTHOR INFORMATION

### Corresponding Author

\*E-mail: ajavey@berkeley.edu.

### Author Contributions

<sup>†</sup>These authors contributed equally.

### Notes

The authors declare no competing financial interest.

## ACKNOWLEDGMENTS

This work at the University of California, Berkeley was supported by NSF Nanomanufacturing Systems for Mobile Computing and Energy Technologies (NASCENT) Center and at Stanford University was supported by the National Institutes of Health grant no. P01 HG000205. The sensor fabrication was performed in the Electronic Materials (E-MAT) laboratory funded by the Director, Office of Science, Office of Basic Energy Sciences, Material Sciences and Engineering Division of the U.S. Department of Energy under contract no. DE-AC02-05CH11231. K.C. acknowledges support from the Robert N. Noyce Fellowship in Microelectronics. The authors thank H.W.W.N. for her assistance.

## REFERENCES

- (1) Young, V.; Garza, C. *Dietary Reference Intakes for Calcium, Phosphorus, Magnesium, Vitamin D and Fluoride*. Standing Committee on the Scientific Evaluation of Dietary Reference Intakes, Food and Nutritional Board, Institute of Medicine; National Academy Press: Washington, DC, 1997.
- (2) Robertson, W. G.; Marshall, R. W.; Bowers, G. N. Ionized Calcium in Body Fluids. *CRC Crit. Rev. Clin. Lab. Sci.* **1981**, *15*, 85–125.
- (3) Relman, R. S. Metabolic Consequences of Acid-Base Disorders. *Kidney Int.* **1972**, *1*, 347–359.



- (4) Maalouf, N. M.; Cameron, M. A.; Moe, O. W.; Sakhaee, K. Metabolic Basis for Low Urine pH in Type 2 Diabetes. *Clin. J. Am. Soc. Nephrol.* **2010**, *5*, 1277–1281.
- (5) Schmid-Wendtner, M. H.; Korting, H. C. The pH of the Skin Surface and its Impact on the Barrier Function. *Skin Pharmacol. Physiol.* **2006**, *19*, 296–302.
- (6) Bandodkar, A. J.; Jeerapan, I.; Wang, J. Wearable Chemical Sensors: Present Challenges and Future Prospects. *ACS Sens.* **2016**, *1*, 464–482.
- (7) Kim, D. H.; Lu, N. S.; Ma, R.; Kim, Y. S.; Kim, R. H.; Wang, S. D.; Wu, J.; Won, S. M.; Tao, H.; Islam, A.; Yu, K. J.; Kim, T. I.; Chowdhury, R.; Ying, M.; Xu, L. Z.; Li, M.; Chung, H. J.; Keum, H.; McCormick, M.; Liu, P.; Zhang, Y. W.; Omenetto, F. G.; Huang, Y. G.; Coleman, T.; Rogers, J. Epidermal Electronics. *Science* **2011**, *333*, 838–843.
- (8) Wang, C.; Hwang, D.; Yu, Z.; Takei, K.; Park, J.; Chen, T.; Ma, B.; Javey, A. User-Interactive Electronic Skin for Instantaneous Pressure Visualization. *Nat. Mater.* **2013**, *12*, 899–904.
- (9) Schwartz, G.; Tee, B. C. K.; Mei, J.; Appleton, A. L.; Kim, D. H.; Wang, H.; Bao, Z. Flexible Polymer Transistors with High Pressure Sensitivity for Application in Electronic Skin and Health Monitoring. *Nat. Commun.* **2013**, *4*, 1859.
- (10) Xu, S.; Zhang, Y.; Jia, L.; Mathewson, K. E.; Jang, K.; Kim, J.; Fu, H.; Huang, X.; Chava, P.; Wang, R.; Bhole, S.; Wang, L.; Na, Y. J.; Guan, Y.; Flavin, M.; Han, Z.; Huang, Y.; Rogers, J. A. Soft Microfluidic Assemblies of Sensors, Circuits, and Radios for the Skin. *Science* **2014**, *344*, 70–74.
- (11) Kaltenbrunner, M.; Sekitani, T.; Reeder, J.; Yokota, T.; Kuribara, K.; Tokuhara, T.; Drack, M.; Schwodiauer, R.; Graz, I.; Bauer Gogonea, S.; Bauer, S.; Someya, T. An Ultra-Lightweight Design for Imperceptible Plastic Electronics. *Nature* **2013**, *499*, 458–463.
- (12) Tee, B. C. K.; Chortos, A.; Berndt, A.; Nguyen, A. K.; Tom, A.; McGuire, A.; Lin, Z. C.; Tien, K.; Bae, W.; Wang, H.; Mei, P.; Chou, H.; Cui, B.; Deisseroth, K.; Ng, T. N.; Bao, Z. A Skin-Inspired Organic Digital Mechanoreceptor. *Science* **2015**, *350*, 313–316.
- (13) Takei, K.; Honda, W.; Harada, S.; Arie, T.; Akita, S. Flexible and Wearable Human-Interactive Health-Monitoring Devices. *Adv. Healthcare Mater.* **2015**, *4*, 487–500.
- (14) Chen, K.; Gao, W.; Emaminejad, S.; Kiriya, D.; Ota, H.; Nyein, H. Y. Y.; Takei, K.; Javey, A. Printed Carbon Nanotube Electronics and Sensor Systems. *Adv. Mater.* **2016**, *28*, 4397–4414.
- (15) Huang, X.; Liu, Y. H.; Chen, K. L.; Shin, W. J.; Lu, C. J.; Kong, G. W.; Patnaik, D.; Lee, S. H.; Cortes, J. F.; Rogers, J. A. Stretchable, Wireless Sensors and Functional Substrates for Epidermal Characterization of Sweat. *Small* **2014**, *10*, 3083–3090.
- (16) Curto, V. F.; Fay, C.; Coyle, S.; Byrne, R.; O'Toole, C.; Barry, C.; Hughes, S.; Moyna, N.; Diamond, D.; Benito-Lopez, F. Real-time Sweat pH Monitoring Based on a Wearable Chemical Barcode Microfluidic Platform Incorporating Ionic Liquids. *Sens. Actuators, B* **2012**, *171–172*, 1327–1334.
- (17) Sonner, Z.; Wilder, E.; Heikenfeld, J.; Kasting, G.; Beyette, F.; Swaile, D.; Sherman, F.; Joyce, J.; Hagen, J.; Kelley-Loughnane, N.; Naik, R. The Microfluidics of the Eccrine Sweat Gland, Including Biomarker Partitioning, Transport, and Biosensing Implications. *Biomicrofluidics* **2015**, *9*, 031301.
- (18) Bandodkar, A. J.; Hung, V. W. S.; Jia, W.; Valdes-Ramírez, G.; Windmiller, J. R.; Martinez, A. G.; Ramírez, J.; Chan, G.; Kerman, K.; Wang, J. Tattoo-based Potentiometric Ion-Selective Sensors for Epidermal pH Monitoring. *Analyst* **2013**, *138*, 123–128.
- (19) Bandodkar, A. J.; Molinnus, D.; Mirza, O.; Guinovart, T.; Windmiller, J. R.; Valdés-Ramírez, G.; Andrade, F. J.; Schöning, M. J.; Wang, J. Epidermal Tattoo Potentiometric Sodium Sensors with Wireless Signal Transduction for Continuous Noninvasive Sweat Monitoring. *Biosens. Bioelectron.* **2014**, *54*, 603–609.
- (20) Jia, W.; Bandodkar, A. J.; Valdes-Ramírez, G.; Windmiller, J. R.; Yang, Z.; Ramírez, J.; Chan, G.; Wang, J. Electrochemical Tattoo Biosensors for Real-Time Noninvasive Lactate Monitoring in Human Perspiration. *Anal. Chem.* **2013**, *85*, 6553–6560.
- (21) Rose, D. P.; Ratterman, M.; Griffin, D. K.; Hou, L.; Kelley-Loughnane, N.; Naik, R. K.; Hagen, J. A.; Papautsky, I.; Heikenfeld, J. Adhesive RFID Sensor Patch for Monitoring of Sweat Electrolytes. *IEEE Trans. Biomed. Eng.* **2014**, *62*, 1457–1465.
- (22) Schazmann, B.; Morris, D.; Slater, C.; Beirne, S.; Fay, C.; Reuveny, R.; Moyna, N.; Diamond, D. A Wearable Electrochemical Sensor for the Real-Time Measurement of Sweat Sodium Concentration. *Anal. Methods* **2010**, *2*, 342–348.
- (23) Kim, J.; Araujo, W. R.; Samek, I. A.; Bandodkar, A. J.; Jia, W.; Brunetti, B.; Paixão, T. R. L. C.; Wang, J. Wearable Temporary Tattoo Sensor for Real-time Trace Metal Monitoring in Human Sweat. *Electrochem. Commun.* **2015**, *51*, 41–45.
- (24) Gao, W.; Nyein, H. Y. Y.; Shahpar, Z.; Fahad, H. M.; Chen, K.; Emaminejad, S.; Gao, Y.; Tai, L.-C.; Ota, H.; Wu, E.; Bullock, J.; Zeng, Y.; Lien, D.-H.; Javey, A. Wearable Microsensor Array for Multiplexed Heavy Metal Monitoring of Body Fluids. *ACS Sens.* **2016**, DOI: 10.1021/acssensors.6b00287.
- (25) Lee, H.; Choi, T. K.; Lee, Y. B.; Cho, H. R.; Ghaffari, R.; Wang, L.; Choi, H. J.; Chung, T. D.; Lu, N.; Hyeon, T.; Choi, S. H.; Kim, D. H. A Graphene-Based Electrochemical Device with Thermoresponsive Microneedles for Diabetes Monitoring and Therapy. *Nat. Nanotechnol.* **2016**, *11*, 566–572.
- (26) Shortreed, M.; Kopelman, R.; Kuhn, M.; Hoyland, B. Fluorescent Fiber-Optic Calcium Sensor for Physiological Measurements. *Anal. Chem.* **1996**, *68*, 1414–1418.
- (27) Shalom, S.; Strinkovski, A.; Peleg, G.; Druckmann, S.; Krauss, A.; Lewis, A.; Linial, M.; Ottolenghi, M. An Optical Submicrometer Calcium Sensor with Conductance Sensing Capability. *Anal. Biochem.* **1997**, *244*, 256–259.
- (28) Bühlmann, P.; Pretsch, E.; Bakker, E. Carrier-Based Ion-Selective Electrodes and Bulk Optodes. 2. Ionophores for Potentiometric and Optical Sensors. *Chem. Rev.* **1998**, *98*, 1593–1687.
- (29) Prestipino, G.; Falugi, C.; Falchetto, R.; Gazzotti, P. The Ionophore ETH 129 as  $\text{Ca}^{2+}$  Translocator in Artificial and Natural Membranes. *Anal. Biochem.* **1993**, *210*, 119–122.
- (30) Bedlechowicz, I.; Sokalski, T.; Lewenstamb, A.; Maj-zurawska, M. Calcium Ion-Selective Electrodes under Galvanostatic Current Control. *Sens. Actuators, B* **2005**, *108*, 836–839.
- (31) Lindfors, T.; Ivaska, A. Calcium-Selective Electrode Based on Polyaniline Functionalized with Bis[4-(1,1,3,3-tetramethylbutyl)-phenyl]phosphate. *Anal. Chim. Acta* **2001**, *437*, 171–182.
- (32) Gao, W.; Emaminejad, S.; Nyein, H. Y. Y.; Challa, S.; Chen, K.; Peck, A.; Fahad, H. M.; Ota, H.; Shiraki, H.; Kiriya, D.; Lien, D.-H.; Brooks, G. A.; Davis, R. W.; Javey, A. Fully Integrated Wearable Sensor Arrays for Multiplexed *In Situ* Perspiration Analysis. *Nature* **2016**, *529*, 509–514.
- (33) Tiwari, A.; Patra, H. K.; Turner, A. P. F. *Advanced Bioelectronic Materials*; Scrivener: Beverly, MA, 2015; p 107.
- (34) Guinovart, T.; Crespo, G. A.; Rius, F. X.; Andrade, F. J. A Reference Electrode Based on Polyvinyl Butyral (PVB) Polymer for Decentralized Chemical Measurements. *Anal. Chim. Acta* **2014**, *821*, 72–80.
- (35) Baker, L. B.; Stofan, J. R.; Lukaski, H. C.; Horswill, C. A. Exercise-Induced Trace Mineral Element Concentration in Regional versus Whole-Body Wash-Down Sweat. *Int. J. Sport Nutr. Exercise Metab.* **2011**, *21*, 233–239.
- (36) Katz, S.; Schoni, M. H.; Bridges, M. A. The Calcium Hypothesis of Cystic Fibrosis. *Cell Calcium* **1984**, *5*, 421–440.
- (37) Verde, T.; Shephard, R. J.; Corey, P.; Moore, R. Sweat Composition in Exercise and in Heat. *J. Appl. Physiol.* **1982**, *53*, 1540–1545.
- (38) Shirreffs, S. M.; Maughan, R. J. Whole Body Sweat Collection in Humans: An Improved Method with Preliminary Data on Electrolyte Content. *J. Appl. Physiol.* **1997**, *82*, 336–341.
- (39) Ansaldi, A.; Epstein, S. I. Calcium Ion-Selective Electrode in which a Membrane Contacts Graphite directly. *Anal. Chem.* **1973**, *45*, 595–596.
- (40) Kent, P.; Bunce, S. C.; Bailey, R. A.; Aikens, D. A. Interference by Polyamines in the Measurement of Magnesium Ion at Physiological



pH with the Divalent Cation-Selective Electrode. *Anal. Biochem.* **1974**, *62*, 75–80.

(41) Matousek, J. L.; Campbell, K. L. A Comparative Review of Cutaneous pH. *Adv. Vet. Dermatol.* **2002**, *13*, 293–300.

(42) Suzuki, H.; Shiroishi, H. Microfabricated Liquid Junction Ag/AgCl Reference Electrode and Its Application to a One-Chip Potentiometric Sensor. *Anal. Chem.* **1999**, *71*, S069–S075.

(43) Sprigle, S.; Linden, M.; McKenna, D.; Davis, K.; Riordan, B. Clinical Skin Temperature Measurement to Predict Incipient Pressure Ulcers. *Adv. Skin Wound Care* **2001**, *14*, 133–137.

# Supporting Information of

## A Wearable Electrochemical Platform for Non-Invasive Simultaneous Monitoring of $\text{Ca}^{2+}$ and pH

*Hnin Y. Y. Nyein<sup>1,2,3‡</sup>, Wei Gao<sup>1,2,3‡</sup>, Ziba Shahpar<sup>1</sup>, Sam Emaminejad<sup>1,2,3,4</sup>, Samyuktha Challa<sup>4</sup>, Kevin Chen<sup>1,2,3</sup>, Hossain M. Fahad<sup>1,2</sup>, Li-Chia Tai<sup>1,3</sup>, Hiroki Ota<sup>1,2,3</sup>, Ronald W. Davis<sup>4</sup>, Ali Javey<sup>1,2,3\*</sup>*

<sup>1</sup>Department of Electrical Engineering and Computer Sciences, University of California, Berkeley, California 94720, USA.

<sup>2</sup>Berkeley Sensor and Actuator Center, University of California, Berkeley, California 94720, USA.

<sup>3</sup>Materials Sciences Division, Lawrence Berkeley National Laboratory, Berkeley, California 94720, USA.

<sup>4</sup>Stanford Genome Technology Center, Stanford School of Medicine, Palo Alto, California 94304, USA

### **Table of Contents:**

Figure S1. Long-term stability of  $\text{Ca}^{2+}$  and pH sensors.

Figure S2. pH sensor tested with Ag/AgCl and PVB reference electrodes in varying  $[\text{Cl}^-]$  solutions.

Figure S3. Temperature dependence of  $\text{Ca}^{2+}$  and pH sensor.

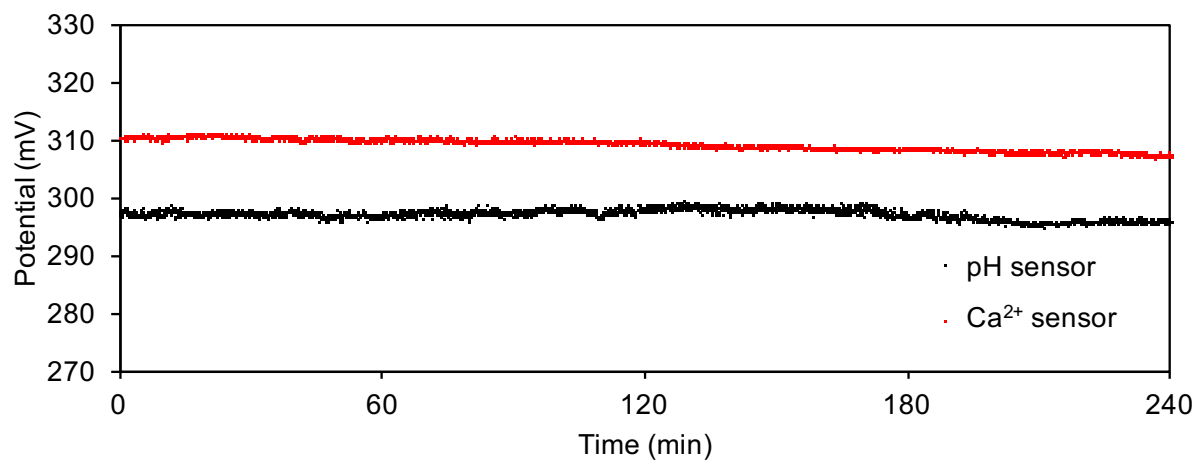


Figure S1. Long-term stability of Ca<sup>2+</sup> and pH sensors in 0.01 M acetate buffer containing 1 mM CaCl<sub>2</sub> in 4 hours. Potential is reported with respect to a standard Ag/AgCl reference electrode.

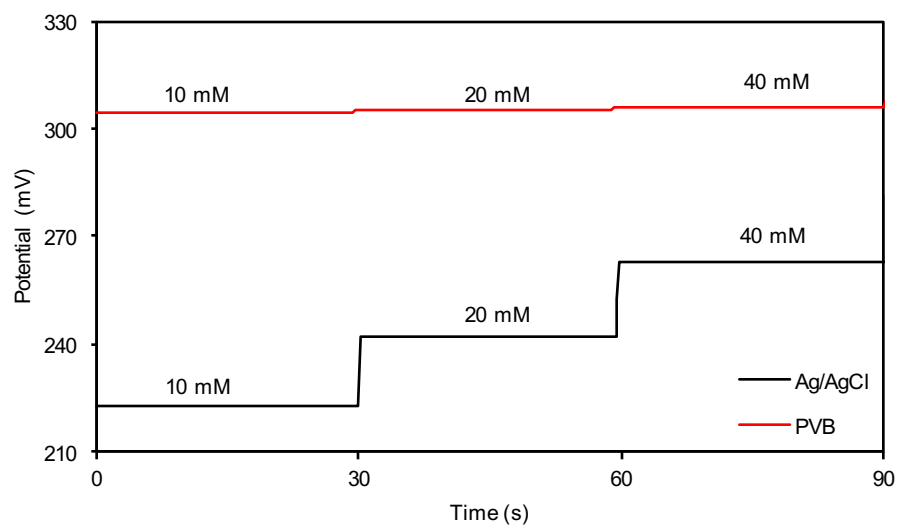


Figure S2. pH sensor tested with Ag/AgCl and PVB reference electrodes in McIlvaine's buffer of pH 5.0 with varying concentration of NaCl. Potential is reported with respect to a standard Ag/AgCl reference electrode.



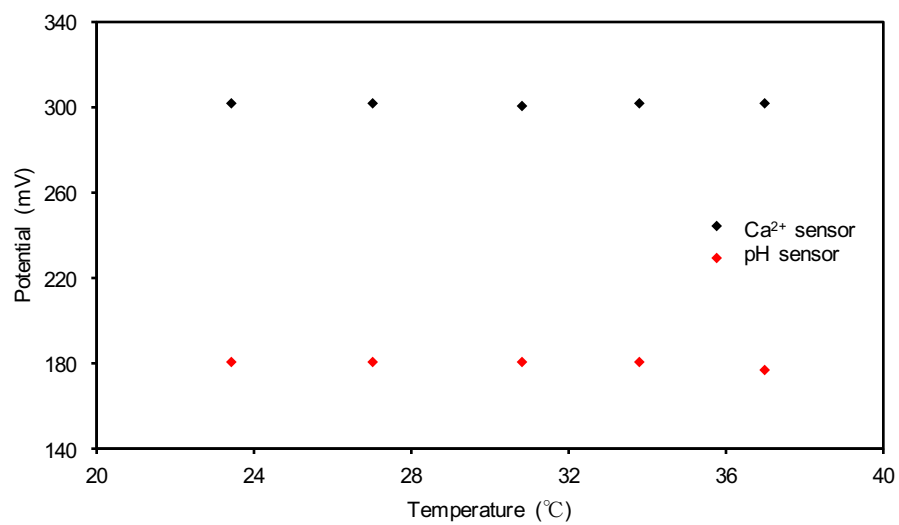


Figure S3. Temperature dependence of  $\text{Ca}^{2+}$  and pH sensor in a solution containing 0.5 mM  $\text{Ca}^{2+}$  in McIlvaine's buffer of pH 5.0.